Large-Aperture, Plasma-Assisted Deposition of Inertial Confinement Fusion Laser Coatings

Introduction

As inertial confinement fusion (ICF) laser systems continue to evolve, the need for large-aperture optical coatings suitable for use in vacuum continues to increase.[1,2] Laser pulses that are temporally compressed to the picosecond scale or shorter must propagate in vacuum because of *B*-integral and self-focusing effects.[3] While reducing the oxygen backfill during silica evaporation may make multilayer coatings less tensile, traditional electron-beam–deposited coatings tend to experience tensile stress failures in vacuum environments.[4] More-energetic techniques such as magnetron sputtering, ion-beam sputtering, and ion-assisted deposition result in films with compressive stresses, but these techniques tend to have difficulties with low laser-damage resistance, high film stresses, and/or scale-up to large apertures.[2,5,6] It is essential for ICF laser-system components to establish a coating process that is stable, with a low-compressive stress in vacuum, and a high laser-damage resistance, particularly for picosecond-scale pulses.

This effort focuses on the development and implementation of a hafnia/silica coating process for meter-scale optical coatings with a controlled compressive stress and high laser-damage resistance. Establishing a low-magnitude compressive stress in the coating is critical for large optics to avoid tensile stress failures while maintaining the optical surface figure without unacceptably thick, heavy, and expensive substrates. A plasma source utilizing a lanthanum hexaboride cathode (LaB_6) was selected for modification of the film because of its low defect density, smooth resulting film structure, and high plasma current necessary for densification of hafnia.[7,8] In this article, results using a single plasma source to modify electron-beam–deposited coatings are presented. Deposition conditions were modified to provide controlled film stresses and high laser-damage thresholds under various wavelengths and pulse durations. This work was then adapted to develop and implement a dual-plasma-source system in a 72-in. coating chamber, suitable for processing meter-scale optics. This process has been used to coat a 0.8-m mirror for use in vacuum at 1053 nm with a 10-ps pulse duration on the OMEGA EP Laser System.

Background

Ion-assisted deposition (IAD) and plasma-assisted deposition, or plasma–ion-assisted deposition (PIAD), have been used to create environmentally stable optical coatings, coating processes suitable for use on temperature-sensitive substrates, and more mechanically durable coatings.[9–12] These processes utilize an ionized gas that is accelerated with a magnetic field toward the substrate surface during the coating process. Some ion sources can operate on O_2 gas alone, while others require the addition of a neutral gas, such as argon.[7,8,10,13,14]

Using ion and plasma sources to modify a standard electron-beam evaporation process provides a significant benefit by introducing many additional control variables that may be used to influence film properties such as humidity stability, film stress, mechanical durability, and material refractive indices. Evaporation is a low-energy deposition process, leading to porous coatings that adsorb moisture, making the optical thickness of the film, as well as the coating stress, a function of the relative humidity in the use environment.[12] Variables such as beam voltage, current, gas selection, and gas flow, in addition to source location and pointing, can be utilized to alter these film properties by transferring momentum from incident ions to the condensing film, altering the structure, and collapsing the pores present in the coating.[15] The introduction of these variables requires care in determining the appropriate operating conditions for each to achieve the desired film performance without negatively influencing other film characteristics.

The choice of gas used in a plasma or ion process can have a significant impact on the resulting film densification. Ions with greater mass provide a correspondingly greater momentum, resulting in additional influence on the condensing film structure.[10,16] The deposition of oxide films by evaporation typically requires the addition of oxygen to the vacuum environment, introducing it directly into the chamber, where it is dispersed. By passing the oxygen through an ion or plasma source, the gas is ionized and accelerated, imparting momentum to the oxygen molecules, leading to densification of the growing film

as the oxygen impacts the surface. As greater densification is required, more argon may be used in the plasma to benefit from its greater atomic mass. If a further increase in momentum is required, higher-atomic-mass gases such as krypton or xenon may be used to provide additional ion momentum. As the relative content of oxygen is decreased, however, the film must be carefully evaluated to prevent an increase in optical absorption, leading to a reduced laser-damage threshold.

Plasma or ion-beam current is simply related to the flow of ions, each of which carries a charge equivalent to the charge of an electron. Increased current in a plasma- or ion-assisted process tends to provide greater densification of the coating being deposited without the risk associated with increased absorption, as is the case with increased ion voltage. Since current will influence the film density, it will also play a role in the ultimate stress achieved in the film. In particular, the impact of ions modifies the film porosity and reduces or eliminates the exchange of water vapor, leading to changes in film stress.[4,15]

The operating voltage of a plasma source determines the energy of an arriving ion at the substrate surface. By increasing the source voltage, higher ion energies and a correspondingly greater densification of the film structure are achieved; however, ions with too high an energy may break atomic bonds in the film, leading to damage of the coating material and the formation of localized absorption sites. Ion voltage may also influence crystalline content in the film since the film structure exhibits characteristics of deposition at a higher temperature with an increased crystallite size; surface roughness and film stress are also modified.[17] Ion beams and plasmas impart energy to the condensing film, causing the displacement of surface atoms and the compaction of the film structure. Using ions to assist the deposition process may lead to energies at the surface equivalent to deposition temperatures in excess of 10^6 K (Ref. 18). This enables one to continuously modify the film structure from a porous, columnar structure realized with electron-beam evaporation to a highly crystalline film in an extremely compressive state resulting from significant ion impingement. This change in film structure is described by structure-zone models with equivalent deposition temperatures.[19–21] By adjusting the characteristics of the plasma flux and the evaporant conditions, the desired film stress and density may be achieved.

Coating stress is comprised of intrinsic and thermal stresses. The influence of energetic deposition is such that the intrinsic stress becomes significantly more important, able to balance or dominate the thermal stresses present in the film resulting from the differing coefficients of thermal expansion for coating and substrate materials when depositing at elevated temperatures. The relationship between the film stress and the substrate surface deflection is described by Stoney's equation[22]

$$\sigma = \frac{E_s t_s^2}{6(1-\nu_s) t_f R}, \tag{1}$$

where σ is the stress in the film, R is the radius of curvature of the surface, E_s is Young's modulus of the substrate, ν_s is Poisson's ratio for the substrate, and t_f and t_s are the thickness of the film and substrate, respectively. It should be noted that Stoney's equation is an approximation, suitable when $t_f \ll t_s$. Plasma-assisted deposition controls film properties in a way that the deposition process may be tuned for each substrate material with its corresponding thermal stresses by altering the intrinsic stress of the film. The degree of control achievable with a plasma-assisted process will determine the magnitude of the film stress that can be realized and, consequently, the substrate thickness necessary to meet the required surface flatness for an optical component.

The distribution of the ion flux from an ion or plasma source may be modeled much like a deposition source, using a cosine distribution.[23,24] A primary advantage of plasma sources is that the extraction coil enables one to alter the source flux by changing the strength of the magnetic field in the extractor coil.[25] Also, unlike deposition, the influence of the impinging ions is not simply a linear process. To a large extent is a thresholding process, where a minimum ion flux is required to achieve film densification.[6] The primary goal in this work, however, is the establishment of a low-magnitude compressive-film stress, without the need for complete densification. The source placement and flux-distribution tuning must be performed in such a manner that the film densification and corresponding structure are controlled over the aperture of the substrates.

Experimental Procedure

An initial series of coatings was prepared in a cryo-pumped, 56-in. coating chamber equipped with quartz heater lamps, dual electron-beam guns, multipoint quartz crystal monitoring, and planetary substrate rotation as shown in Fig. 124.21. Granular silicon dioxide was evaporated from a continuously rotating pan, while hafnium metal was deposited in the presence of oxygen from a stationary six-pocket electron-beam gun to form hafnium dioxide. A single Satis PDS plasma source was installed in the chamber at a radius of 15 in. from chamber center to provide a uniform ion flux over the aperture of the substrate.

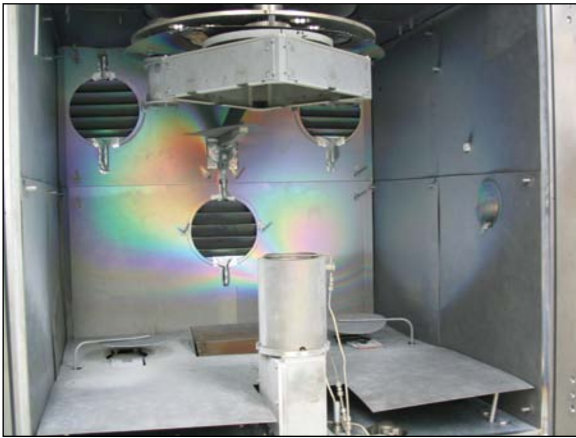

G9089JR

Figure 124.21
The 56-in. coating chamber with planetary rotation, dual electron-beam guns, and a single Satis PDS plasma source. The plasma source is positioned off-center in the chamber to provide a more-uniform plasma flux over the substrate aperture.

The primary concern with energetically assisting the deposition process for high-peak-power laser applications is that the laser-damage threshold will be compromised, leading to reduced fluence capabilities for the laser.[2] Hafnia monolayers were deposited on cleaved float glass with an optical thickness of four quarter-waves at 351 nm to form an absentee layer that minimizes the influence of the standing-wave electric field in the film. The cleaved-glass substrate eliminates the effects of substrate fabrication and cleaning processes on laser-damage thresholds.[26] The plasma settings for the initial samples were 140 to 180 V/35 A (acceleration voltage/beam current), a nominal 10 sccm of argon gas surrounding the LaB_6 cathode in the plasma source controlled to maintain constant beam current/voltage, and 50 sccm of O_2 gas injected into the plasma using a gas-distribution ring on the top of the source. Chamber pressure was controlled through oxygen backfill to maintain a constant pressure of 4.0×10^{-4} Torr. Laser-damage testing was performed in a standard 1:1 testing configuration at 351 nm at a 0.5-ns pulse duration.[27] Finally, x-ray diffraction (XRD) measurements of the hafnia films were collected using a Philips Materials Research diffractometer (MRD) with a CuKα source to evaluate the crystallinity of the hafnia structure. The coated samples were oriented in a near-grazing incidence configuration, with an incident angle $\theta = 2.2°$ and a diffracted angle 2θ incremented in steps of 0.02°, with a 13-s integration time at each position.

The film stress in hafnia monolayers was also evaluated as a function of plasma-assist voltage since this is the primary benefit for large-aperture laser coatings. Hafnia layers with a 140-nm thickness were deposited on 25-mm-diam × 1-mm-thick BK7 substrates. Surface flatness was measured using a Zygo New View interferometer at controlled relative humidities of 0% and 40%, measuring the uncoated surface of the substrate to avoid the influence of phase effects from the coating. The optics were supported horizontally on a three-point mounting fixture, using equally spaced ball bearings placed at 65% of the radius of the substrate to minimize deflection caused by mounting. The resulting stress in the hafnia films was evaluated as a function of plasma voltage to determine appropriate operating conditions for low-stress coatings.

Development of the plasma-assist process continued with the deposition of multilayer high-reflector coatings using a broad range of deposition conditions, including variations of plasma voltage, current, gas flows, deposition rates, substrate temperature, and chamber pressure. The influence of the deposition conditions on film stress and laser-damage resistance was evaluated to determine optimal deposition conditions. Selected deposition processes were used to deposit high-reflector coatings centered at λ_0 = 1053 nm on 310-mm-diam × 14-mm-thick fused-silica substrates for evaluation on an 18-in. Zygo interferometer and a large-aperture laser conditioning station according to National Ignition Facility (NIF) protocol.[28]

Finally, the plasma-assist process was installed in a 72-in. coating chamber (as shown in Fig. 124.22) utilizing two Thin

G9090JR

Figure 124.22
A Thin Film Solutions Ltd. dual-plasma-source system installed in LLE's 72-in. electron-beam evaporation system. The plasma sources provide a high ion flux over the entire surface of the meter-scale substrates.

Films Solutions Ltd. plasma sources, based on the original Satis PDS source design.[8,25] Two sources were implemented to ensure adequate plasma flux over the surface of a large optic, given a significantly greater source-to-substrate distance than that in the 56-in. coating chamber, as well as to provide redundancy in the event of a source failure. Custom control software was developed to ramp the source in a series of steps to prevent the poisoning of one source cathode by the operation of the second source. The plasma sources were installed at a radial position of 8.3 in. from chamber center, compromising between maximum ion flux and uniformity. Additional mounting locations were machined in the chamber base plate to provide the ability to tune the flux distribution over the substrate aperture as needed. Uniformity masks were reconfigured to avoid significant impingement of the plasma on the film-correction masks.[23] The sources were operated at 145 V with a beam current of 20 A each, introducing 50 sccm of O_2 during hafnia deposition and 15 sccm of O_2 during silica deposition. Cathode temperatures were kept as low as possible by minimizing the rf power to reduce film defects caused by cathode ejections. Interaction between the sources was determined to be negligible during operation.

Results

Throughout this effort to develop plasma-assisted–deposition processes, the plasma conditions (current, voltage, and gas flows) were modified, as well as chamber conditions (oxygen backfill, deposition rates, and substrate temperature). A qualitative understanding of the influence of each parameter is of primary importance since the process space becomes much larger as the number of process variables is increased. Different chamber configurations will require different operational parameters since the influence of a given plasma voltage, current, and gas flow will be strongly dependent on the source location, distance to the substrate, substrate size, and the substrate motion.

As the use of different gas flows and corresponding chamber pressures was evaluated, one consideration was where to introduce the gas. Oxygen is typically introduced during reactive electron-beam deposition, but the inclusion of a plasma-assist source allows one to introduce some or all of the oxygen through the plasma source. Deposition tests were undertaken with oxygen introduced in the chamber or through the plasma source at different controlled operating pressures. As shown in Fig. 124.23, as the chamber pressure is increased, there is a greater change in optical thickness of the hafnia coating between 0%- and 40%-relative-humidity environments caused by water movement into the pores of the film. By introducing the oxygen through the plasma source with all other plasma operating conditions constant, film porosity is reduced 30% to 50%.

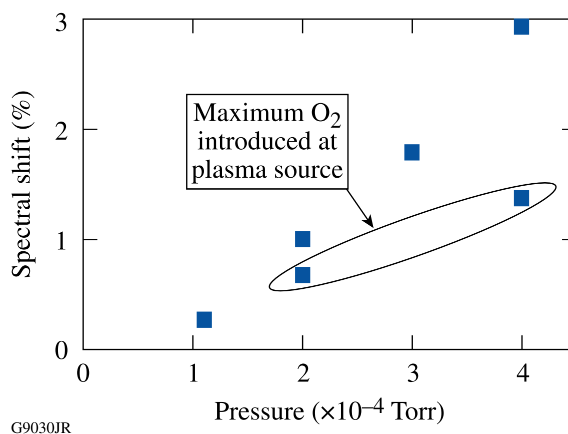

Figure 124.23
Influence of O_2 backfill pressure on the resulting sensitivity of hafnia films to relative humidity. A larger spectral shift between 0% and 40% relative humidity indicates greater film porosity.

It has been found previously that laser-damage thresholds of electron-beam–deposited hafnia improve as the porosity of the film increases.[29,30] The influence of plasma-assisted deposition on the laser-damage threshold of hafnia coatings was explored for 351-nm light. To minimize the influence of substrate preparation on laser-damage thresholds, coatings were deposited on cleaved float-glass surfaces.[26] Laser-damage testing was performed in a standard 1:1 testing configuration at 351 nm at a 0.5-ns pulse duration.[30] Laser-damage characterization at 351 nm provides greater sensitivity to changes in film absorption than evaluation at 1053 nm, which tends to be dominated by film defects. These tests demonstrate minimal rate or plasma-voltage influence over the range of parameters tested, as shown in Fig. 124.24. The relatively insignificant change in laser-damage threshold for a plasma voltage in the range of 140 to 180 V indicates the corresponding change in optical absorption of the film must also be negligible. Since the film is deposited with plasma assist, it has a reduced porosity and a correspondingly greater density than a film deposited at the equivalent pressure by electron-beam evaporation. Additionally, the use of plasma assist makes low-porosity deposition no longer necessary to maintain high-laser-damage resistance.[29,30]

The crystallinity of the hafnia monolayers deposited at 180 V with a 35-A plasma current measured using XRD is shown in Fig. 124.25. The electron-beam–evaporated hafnia exhibits a relatively weak monoclinic crystalline signature, while the crystalline peaks become much more defined as the

ion/evaporant ratio is increased. As the deposition rate of the hafnia is decreased, the relative ion flux is effectively increased and the crystallites grow to approximately 12 nm as calculated using Scherrer's equation.[30,31] This increase in film crystallinity is equivalent to an increased substrate temperature as described in a structure-zone model.[19–21] It was determined in a previous study that a reduction in film crystallinity could be correlated with improved laser-damage thresholds for 351-nm light.[30] This does not appear to hold true for PIAD films based on the results shown in Figs. 124.24 and 124.25.

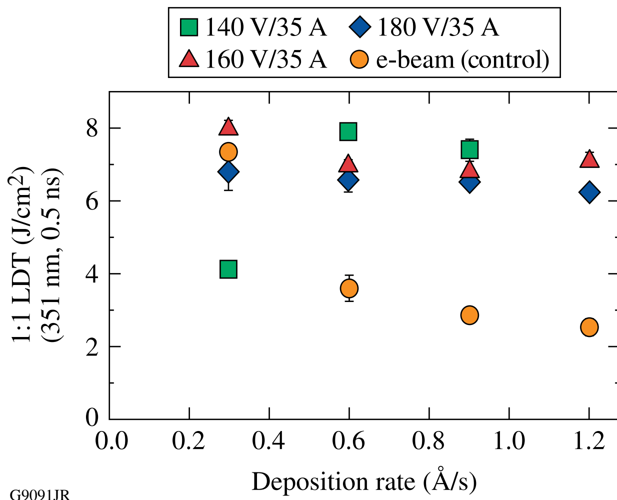

Figure 124.24
Laser-damage thresholds of hafnia deposited with PIAD exhibit minimal deposition-rate dependence, unlike typical electron-beam deposition of hafnia. The control electron-beam coating was deposited with an oxygen backfill pressure of 2×10^{-4} Torr.

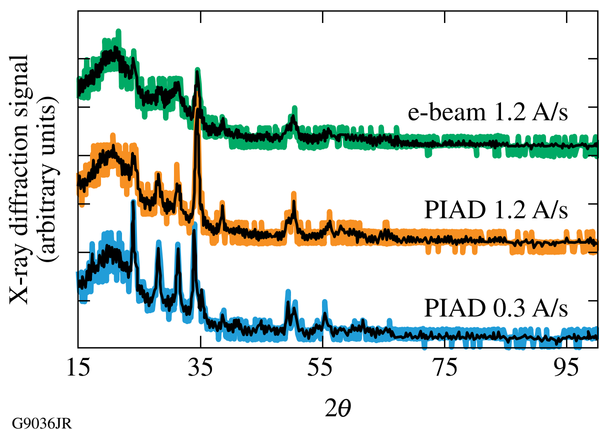

Figure 124.25
X-ray diffraction measurements of hafnia monolayers indicate increasing crystallinity as the plasma/evaporant flux is increased. This may be achieved by increasing the plasma current or decreasing the deposition rate.

The film stress in hafnia monolayers was also evaluated as a function of plasma-assist voltage. Hafnia layers of 140-nm thickness were deposited on 25-mm-diam $\times$ 0.25-mm-thick BK7 substrates. Surface-flatness measurements were performed on a Zygo New View interferometer at relative humidities of 0% and 40%. Using Eq. (1), these measurements were used to calculate the film stress. The resulting stress in the hafnia films is plotted in Fig. 124.26(a) as a function of plasma voltage when operated at 35 A to determine appropriate operating conditions for low-stress coatings. The stress transitioned from a tensile state below 145 V to an increasingly compressive state above this plasma potential. All film stresses for plasma-assisted silica films plotted in Fig. 124.26(b) were found to be compressive, with an increasing compressive stress as the plasma voltage was increased.

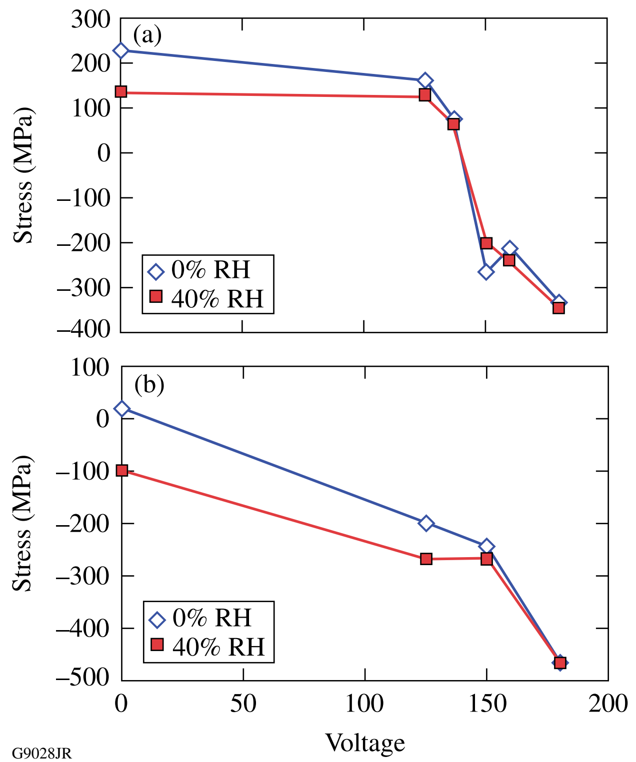

Figure 124.26
(a) Influence of plasma-assist voltage on the stresses in hafnia monolayers. An assist of approximately 145 V at 35 A is sufficient to transition from tensile to compressive stress. (b) Influence of plasma-assist voltage on the stresses in silica monolayers. Note that all silica stresses are compressive, except the evaporated silica (no PIAD) in a dry environment.

Development of the plasma-assist process continued with the deposition of multilayer high-reflector coatings using a broad range of deposition conditions, including variations of plasma voltage, current, gas flows, deposition rates, substrate temperature, and chamber pressure. The influence of the depo-

sition conditions on film stress and laser-damage resistance was evaluated to determine optimal deposition conditions. In general, the addition of energetic ions through PIAD resulted in a more-compressive coating with a reduced sensitivity to relative humidity than a comparable coating produced with only electron-beam evaporation, as shown in Fig. 124.27. The PIAD results shown are from a coating deposited with a 170-V/40-A plasma, leading to greater densification of the film and a reduced sensitivity to humidity. The chamber temperature was adjusted to 140 °C, which is as low as possible while maintaining a controlled, constant temperature during PIAD operation.

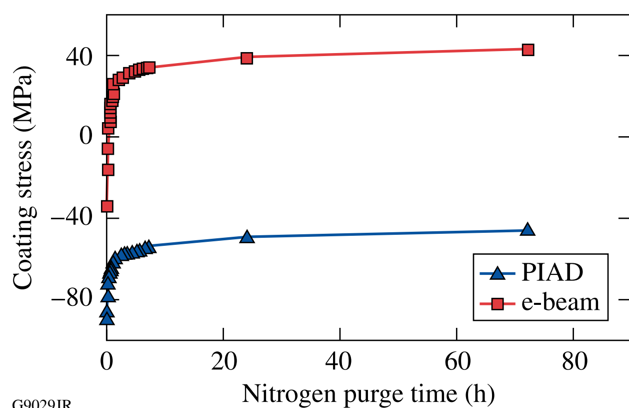

Figure 124.27
Change in film stress for PIAD and electron-beam–deposited coatings as the ambient relative humidity changes from 40% RH to 0% RH. While the % RH of the measurement environment changes almost immediately, the removal of water from the film pores is a much slower process, dependent on the diffusion of water through the film structure. Note that PIAD coatings are more compressive, with a smaller change in film stress as the coating is dried.

The densification of only single materials within multilayer coatings was explored by operation of the plasma source during hafnia or silica layers. Hafnia was considered since it is the primary source of tensile stress, as shown in Fig. 124.26(a). Silica was pursued since it undergoes the most significant change in stress as a function of time.[4] However, the presence of porous layers between dense diffusion barriers led to irregular water penetration around film defects, leading to subsequent spotting of the coating. Furthermore, the argon backfill required to idle the plasma sources resulted in a poorer vacuum during nondensified layers. The densification of alternating layers was determined to be problematic and not pursued further.

Selected deposition processes were used to deposit high-reflector coatings centered at λ_0 = 1053 nm on 310-mm-diam × 14-mm-thick fused-silica substrates for evaluation on an 18-in. Zygo interferometer and large-aperture laser conditioning station according to NIF protocol.[28] As shown in Fig. 124.28, the stress in the electron-beam–deposited coating continued to become more tensile as the coating aged, with changes in film stress apparent more than six months after deposition. PIAD samples 1 and 2 show a film stress that remained constant, within ±10 MPa, over an extended duration. A controlled compressive stress with a magnitude of 20 to 30 MPa is ideal to avoid difficulties arising from tensile-stress failures (crazing), while imparting minimal reflected wavefront deformation caused by stress.

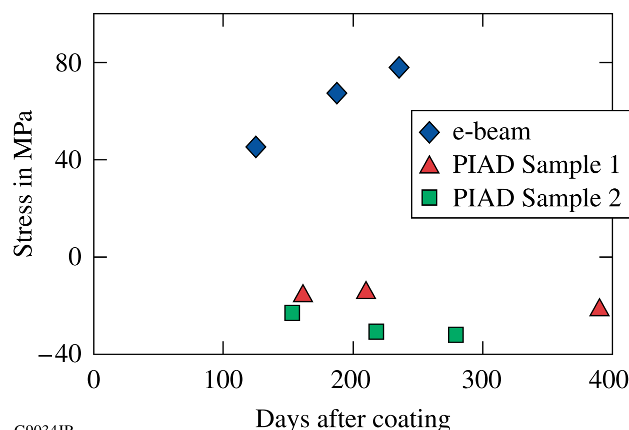

Figure 124.28
Change in film stress for PIAD and electron-beam–deposited coatings at 0% RH as a function of aging. While e-beam–deposited coatings continue to change significantly over periods of months, partially dense PIAD coatings with near-neutral stress maintain a consistent film stress.

The dual-source system was operated at 145 V with a beam current of 20 A from each source, introducing 50 sccm of O_2 during hafnia deposition and 15 sccm of O_2 during silica deposition. Meter-scale high-reflector coatings were produced with a compressive stress of the order of 50 to 80 MPa in a use environment of 0% relative humidity and a laser-damage threshold of 6.7 J/cm^2 at 1053 nm with a pulse length of 10 ps. Laser-damage testing was performed in an ambient humidity environment at 29° incidence. This process was used to fabricate an 0.8-m mirror, designated as SPHR10, on a BK7 substrate for use in vacuum on the OMEGA EP Laser System, as shown in Fig. 124.29. Measurement of the coated surface indicated 0.38 waves peak-to-valley of surface power on a 1064-nm–wavelength interferometer. Measurement of the film stress for BK7 substrates in a dry environment indicated a stable film stress of approximately 50 MPa. The stress aging of the PIAD coating, as shown in Fig. 124.30, indicated that the aging effects typical of evaporated hafnia silica coatings have been effectively eliminated, even for a PIAD coating with significant porosity and humidity susceptibility.[4,28] The

spectral shift in the optical thickness of the coating from a 0%- to 40%-relative-humidity environment was measured as 1.54±0.14% over a 0.9-m aperture, indicating significant but quite uniform film porosity, although the film was more dense than the reference electron-beam–deposited film with a typical 2.7% spectral shift. The consistency of the film porosity, as determined by the spectral shift in different humidity environments, demonstrated that film densification was quite uniform over the substrate aperture, particularly since the film was only partially densified. Laser-damage thresholds for 1053-nm, 1-ns pulses were measured at 22.09 J/cm^2 in a 1:1 defect-targeting mode. The laser-damage threshold for defect-free sites was determined to be 26.67 J/cm^2, indicating a decrease in laser-damage threshold relative to standard evaporated coatings, which tend to be >85 J/cm^2 for defect-free sites.[1,28]

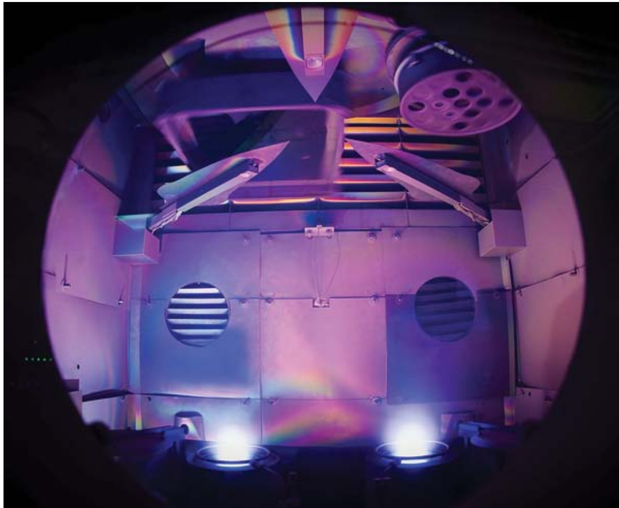

Figure 124.29
The dual-source PIAD system in the 72-in. coating chamber was used to deposit the SPHR10 coating. The plasma effectively fills the entire deposition region, providing a uniform densification of the film over the full aperture of the substrate.

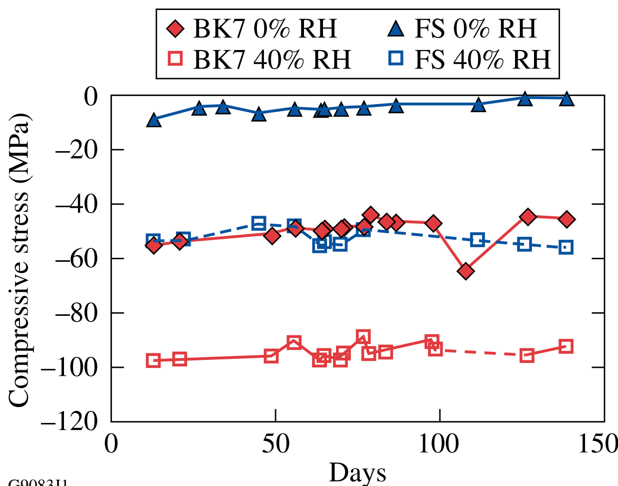

Figure 124.30
Stress-aging measurements of PIAD coatings indicate negligible changes in stress as a function of time after deposition. In comparison, the stress of the e-beam–deposited coating in Fig. 124.28 continues to change significantly six months after deposition.

Conclusions

Plasma-assisted deposition provides a means of tuning the film stress of optical coatings while maintaining high-peak-power laser-damage thresholds. Installation of a plasma-assist process is unique for a given deposition system since each chamber configuration will have a different set of optimal operating parameters for neutral film stress based on the substrate size, rotation geometry, radial position of the source, and other considerations. This development effort provides guidance for tuning the process in different systems. Increased plasma voltage leads to greater densification of the film and a more-compressive film stress. The use of more-energetic oxygen, by ionizing it with a plasma source, leads to a denser coating and improved laser-damage thresholds, particularly for lasers in the ultraviolet region of the spectrum, which are more susceptible to film absorption. Likewise, reduced chamber pressures lead to decreased evaporant scattering and a less-porous film structure.

Controlled compressive film stresses of <50 MPa can be established and maintained in a dry-use environment on fused-silica substrates through plasma-assisted deposition, providing a means of avoiding tensile-stress failures in vacuum while maintaining high-quality surface flatness of the laser components. A plasma-assist process for multilayer coatings has been demonstrated with a low-magnitude compressive stress utilizing a nominal voltage of 145 V during hafnia and silica deposition, with plasma current being adjusted to achieve the desired film stress and densification. This process was integrated in a 72-in. coating chamber to deposit high-precision coatings over 0.9-m aperture optics. The measured laser-damage threshold for a 29° high-reflector coating is 6.7 J/cm^2 (1053 nm, 10-ps pulse) with a compressive film stress of 50 MPa.

ACKNOWLEDGMENT

The authors wish to express their appreciation to Alex Maltsev for his efforts on the fabrication of extremely high quality, high-aspect-ratio substrates for this study. This work was supported by the U.S. Department of Energy Office of Inertial Confinement Fusion under Cooperative Agreement No. DE-FC52-08NA28302, the University of Rochester, and the New York State Energy Research and Development Authority. The support of DOE does not constitute an endorsement by DOE of the views expressed in this article.

REFERENCES

1. J. B. Oliver, A. L. Rigatti, J. D. Howe, J. Keck, J. Szczepanski, A. W. Schmid, S. Papernov, A. Kozlov, and T. Z. Kosc, in *Laser-Induced Damage in Optical Materials: 2005*, edited by G. J. Exarhos *et al.* (SPIE, Bellingham, WA, 2005), Vol. 5991, pp. 394–401.
2. E. Lavastre *et al.*, in *Optical Interference Coatings*, OSA Technical Digest (Optical Society of America, Washington, DC, 2004), p. TuF3.
3. Y.-H. Chuang, L. Zheng, and D. D. Meyerhofer, IEEE J. Quantum Electron. **29**, 270 (1993).
4. H. Leplan *et al.*, J. Appl. Phys. **78**, 962 (1995).
5. D. J. Smith *et al.*, in *Laser-Induced Damage in Optical Materials: 2008*, edited by G. J. Exarhos *et al.* (SPIE, Bellingham, WA, 2008), Vol. 7132, p. 71320E.
6. M. Alvisi *et al.*, Thin Solid Films **358**, 250 (2000).
7. R. Thielsch *et al.*, Thin Solid Films **410**, 86 (2002).
8. F. Placido *et al.*, in *Advances in Thin-Film Coatings for Optical Applications III*, edited by M. J. Ellison (SPIE, Bellingham, WA, 2006), Vol. 6286, p. 628602.
9. H. R. Kaufman and J. M. Harper, in *Advances in Thin Film Coatings for Optical Applications*, edited by J. D. T. Kruschwitz and J. B. Oliver (SPIE, Bellingham, WA, 2004), Vol. 5527, pp. 50–68.
10. M. Kennedy, D. Ristau, and H. S. Niederwald, Thin Solid Films **333**, 191 (1998).
11. E. H. Hirsch and I. K. Varga, Thin Solid Films **69**, 99 (1980).
12. B. G. Bovard, in *Thin Films for Optical Systems*, edited by F. R. Flory (Marcel Dekker, New York, 1995), pp. 117–132.
13. J. R. Kahn, H. R. Kaufman, and V. V. Zhurin, in *46th Annual Technical Conference Proceedings* (Society of Vacuum Coaters, Albuquerque, NM, 2003), pp. 621–625 (Paper 110).
14. D. E. Morton and V. Fridman, in *Proceedings of the 41st Annual Technical Conference of the Society of Vacuum Coaters* (Society of Vacuum Coaters, Albuquerque, NM, 2003), pp. 297–302 (Paper 53).
15. K.-H. Müller, J. Vac. Sci. Technol. A **4**, 184 (1986).
16. J. D. Targove and H. A. Macleod, Appl. Opt. **27**, 3779 (1988).
17. G. Atanassov *et al.*, Thin Solid Films **342**, 83 (1999).
18. H. Kersten *et al.*, Vacuum **46**, 305 (1995).
19. J. V. Sanders, in *Chemisorption and Reactions on Metallic Films*, edited by J. R. Anderson, Physical Chemistry, A Series of Monographs (Academic Press, London, 1971), pp. 1–38.
20. J. A. Thorton, in *Modeling of Optical Thin Films*, edited by M. R. Jacobson (SPIE, Bellingham, WA, 1988), Vol. 821, pp. 95–103.
21. B. A. Movchan and A. V. Demchishin, Fiz. Met. Metalloved **28**, 653 (1969).
22. G. G. Stoney, Proc. R. Soc. Lond. A **82**, 172 (1909).
23. J. B. Oliver and D. Talbot, Appl. Opt. **45**, 3097 (2006).
24. H. R. Kaufman, R. S. Robinson, and R. I. Seddon, J. Vac. Sci. Technol. A **5**, 2081 (1987).
25. D. Gibson, European Patent No. EP 1 154 459 A2 (14 November 2001).
26. S. Papernov, D. Zaksas, J. F. Anzellotti, D. J. Smith, A. W. Schmid, D. R. Collier, and F. A. Carbone, in *Laser-Induced Damage in Optical Materials: 1997*, edited by G. J. Exarhos *et al.* (SPIE, Bellingham, WA, 1998), Vol. 3244, pp. 434–445.
27. S. Papernov and A. W. Schmid, J. Appl. Phys. **82**, 5422 (1997).
28. J. B. Oliver, J. Howe, A. Rigatti, D. J. Smith, and C. Stolz, in *Optical Interference Coatings*, OSA Technical Digest (Optical Society of America, Washington, DC, 2001), p. ThD2.
29. B. Andre, J. Dijon, and B. Rafin, U.S. Patent No. 7,037,595 (2 May 2006).
30. J. B. Oliver, S. Papernov, A. W. Schmid, and J. C. Lambropoulos, in *Laser-Induced Damage in Optical Materials: 2008*, edited by G. J. Exarhos *et al.* (SPIE, Bellingham, WA, 2008), Vol. 7132, p. 71320J.
31. B. D. Cullity, *Elements of X-Ray Diffraction*, 2nd ed. (Addison-Wesley, Reading, MA, 1978).